Validation of the Rotating UT Probe for In-Service Inspections of Freight Solid Axles by Means of the MAPOD Approach

Michele CARBONI*, Stefano CANTINI**, Cristina GILARDONI***
* Dept. Mechanical Engineering, Politecnico di Milano, Via La Masa 1, 20156 Milano, Italy; michele.carboni@polimi.it
** Lucchini RS SpA, Via G. Paglia 45, 24065 Lovere (BG), Italy; s.cantini@lucchinirs.it
*** Gilardoni SpA, Via A. Gilardoni 1, 23826 Mandello del Lario (LC), Italy; gx@gilardoni.it

Abstract. The present scenario of freight applications in Europe is characterized by a trend towards rolling stock renewal and a new approach to periodical inspection and maintenance; this is a consequence of some evidences coming from service and showing potential inconsistency in general safety levels. A specific NDT technique, based on more than 40 years of service experience on passenger wheel-sets inspection, is here proposed for periodical NDT on freight wheel-sets. The ultrasonic testing technique is based on a rotating probe-holder to be applied at the ends of the mounted axle and able to inspect its critical sections with different angled probes. To inspect such critical sections such as press fits and geometrical transitions, the testing device is characterized by a set of ultrasonic transducers emitting longitudinal waves at a typical nominal frequency of 4 MHz and at different angles into the axle. The structural integrity of the wheel-set is then based, together with other factors, on the determination of the Probability of Detection (POD) curve of the rotating probe. An experimental campaign to derive the POD curve can be costly and time consuming, especially considering the determination of its confidence range. For this reason, in the present research, a Model-Assisted POD (MAPOD) approach was considered. Initially, different sets of artificial defects, obtained by EDM, were introduced on the external surface of three solid axles made of A1N steel grade. All the defects were then inspected by a rotating probe, with the aim to derive their response, considering 4 MHz and 2.25 MHz transducers. The effect of the different time of flight characterizing the defects located at the different sections of the axles was, instead, determined by suitable numerical simulations carried out using the CIVA^nde dedicated software package. Combining experimental and numerical results allowed to derive the MAPOD curve for the considered rotating probe with less effort with respect to the traditional experimental approach and to optimize the set-up of the rotating probe itself. As a result, the MAPOD curves of the rotating probe device are compared to the POD of standard UT inspection from axle end and a simulation of the reliability of inspection intervals is presented.

1. Introduction

The present European scenario of freight railways transportation shows a trend toward new procedures for the maintenance of in-service axles, looking for a higher level of safety and, at the same time, an optimization of the total life cycle cost of the wheel-set. Among the traditional inspection techniques, the association of the owners of private wagons has developed its own guidelines for inspecting axles by means of different ultrasonic probes applied from the outer surface of the axles themselves [1]. This technique presents two drawbacks: the need to remove varnish and the need to disassemble bushings and bearings. In particular, the development of a new generation of permanent protective coatings [2] makes it inconvenient even the partial removal to allow UT inspections.

It is worth mentioning that the purpose of in-service inspections is to detect any damage, and subsequent propagation of cracks up to failure, due to characteristic phenomena, such as corrosion-fatigue or impact of the ballast, according to a "Damage Tolerant " approach [3]-[4]. The inspection must therefore be particularly effective in those sections of the axle prone to higher stresses and greater likelihood of damage. Within this background, during the '70s and thanks to the work by the Italian Railways Operator [5], the technique of the rotating probe is employed to inspect solid axles in Italy.

Here is then described an evolution of this NDT technique based on a new rotating probe (Pic. 1a) produced by Gilardoni SpA according to the specifications by Lucchini RS SpA [6]. The probe mounts differently angled transducers (Pic. 1b) so to inspect the critical areas of axles (geometrical transitions and press-fit seats). The traditional limits of this technique are mainly related to the surface condition of the ends of axles.

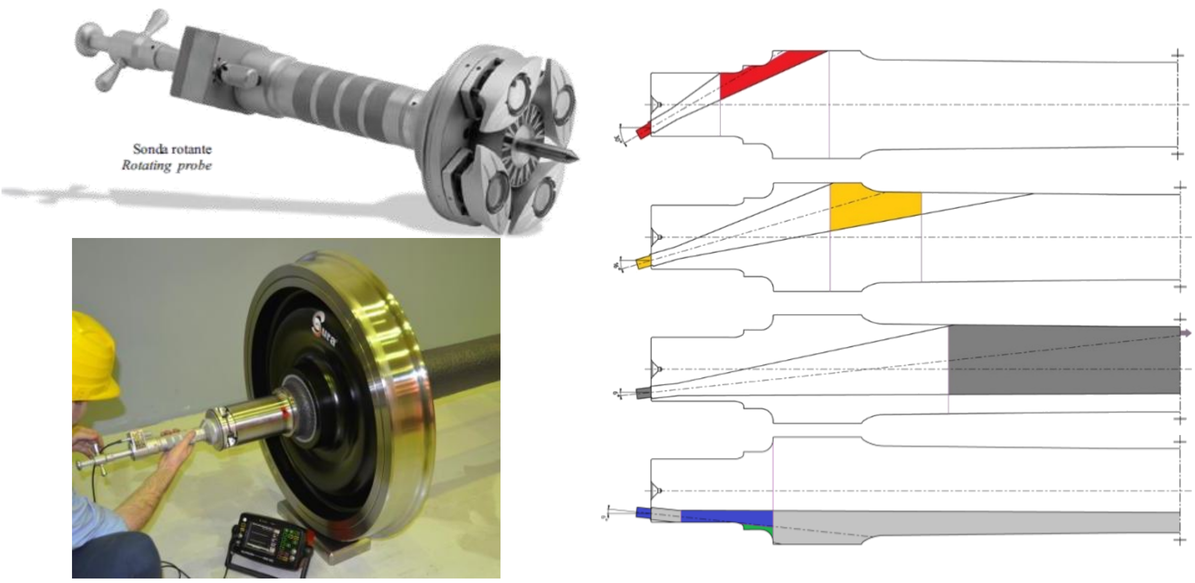

(a) (b)

Pic. 1. The rotating probe for the UT inspection of solid axles.

The structural integrity of solid axles during service is then guaranteed, along with other factors characterizing the Damage Tolerant approach [3]-[4], by the reliable derivation of the “Probability of Detection” (POD) curve [7]-[9] of the rotating probe. Traditionally, such curves are expressed and plotted as a function of a characteristic linear dimension of the defect (depth, length, diameter ...), but they are also a function of many other physical and operational factors. For this reason, very rarely the POD curve determined for a given inspection procedure may be adopted for another one, even if similar. Another critical aspect is that, for reliability and design, what it is needed is a statistical characterization of the largest defect which can be missed and not the smallest defect that can be detected. The POD curves are then often provided along with the 95% confidence band which, to be determined, requires a considerable experimental effort.

In this research work, the possibility of applying the "Model- Assisted Probability of Detection" (MAPOD) approach [10]-[12] to the rotating probe is explored. This approach is very recent and based on the possibility of replacing part of the experimental evidence with the results of numerical analysis, at least for those key parameters that can be defined by effective physical models. It is important to add that the MAPOD approach does not allow removing the entire experimental work required to derive a POD curve, because not all the relevant parameters are, to date, describable by known physical models.

Numerical simulations were here carried out by the CIVA^{nde} 10.1a [13] dedicated software and showed an excellent potential in applying the MAPOD results to the description of the performance of the rotating probe to solid railway axles.

2. Experimental Activity

To evaluate the performance of the rotating probe applied to solid axles made of EA1N steel, three of them were prepared by introducing, in different sections (Pic. 2), a series of artificial defects obtained by EDM. They were characterized by both concave (representative the fretting-fatigue cracks observed at press-fit seats) and convex (representing the classical fatigue cracks observed on the body and along geometrical transitions) shapes. In particular, each section was characterized by three defects of the same shape, but different reflecting area, angularly spaced by 120°.

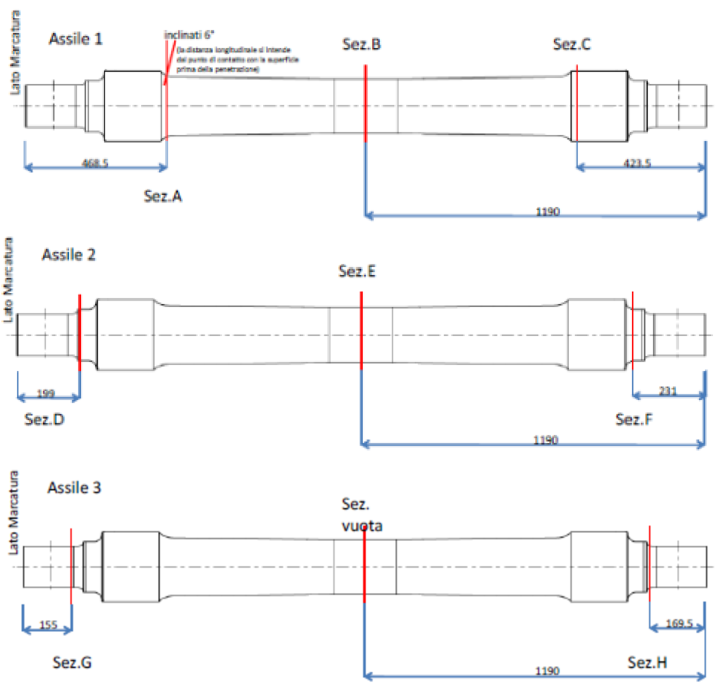

Pic. 2. Sections containing the EDM artificial defects.

All defects were inspected by the rotating probe, connected to a digital Gilardoni RDG500 UT flaw detector, equipped with piezoelectric crystals having diameter of 20 mm and a nominal frequency equal, in two separate test campaigns, to both 4 and 2.25 MHz. Longitudinal waves were employed and their speed was set to 5900 m/s. The refraction angles chosen for the inspection of the different sections containing artificial defects were (Pic. 1b):

- convergent longitudinal waves at 6°: Sec. B, Sec. E
- convergent longitudinal waves at 16°: Sec. A, Sec. C
- convergent longitudinal waves at 30°: Sec. D, Sec. F
- divergent longitudinal waves at 6°: Sec. G, Sec. H

For each defect, the gain level (dB) required to get its response to an amplitude equal to 90% of the screen was recorded. Picture 3a shows, for example, the responses of the defects positioned in sections B and E, which are at the same time of flight (equal to 1190 mm) and contain defects of the same geometry (convex), but different sizes: it is, therefore, possible to consider them in one single set. Picture 3b, instead, shows an example of the results obtained from section G located at a path equal to 155 mm and characterized by concave defects. The diagrams show the size of the defects in terms of the effective reflecting area [14].

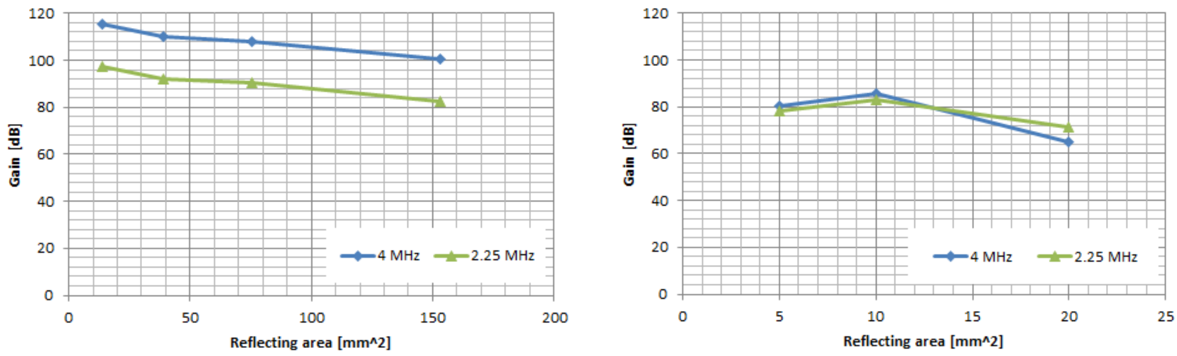

Pic. 3. Ultrasonic responses obtained from Sections B+E and G.

From the observation of Picture 3a, it is possible to note that the 2.25 MHz probe requires levels of sound energy significantly lower than those by the 4 MHz one. Considering, instead, Picture 3b, the energy level for the two frequencies appears to be comparable. Generalizing, Table 1 summarizes the analysis for all the sections containing artificial defects. The obtained results allow proposing a version of the rotating probe optimized in the following way:

1. the inspection of the bearing journal and its transition to the collar (i.e. up to paths equal to 200 mm) should be performed using 4 MHz probes;
2. the inspection of paths longer than 200 mm should be performed using 2 or 2.25 MHz.

Table 1. Summary of the results obtained from solid axles

Section	Path [mm]	Best Frequency [MHz]
B+E	1190	2.25
C	423.5	2.25
F	231	2.25
G	155	Comparable
H	169.5	4

3. MAPOD Approach applied to the Rotating Probe

The achievement of the experimental results described above required some efforts in terms of time and costs and was not enough to define the confidence bounds, too. As mentioned in the Introduction, this problem can be addressed and partially solved by a MAPOD approach. In particular, it relies on the fact that the POD curves are based on statistical distributions that describe the response of the defects, which, in turn, are controlled by a number of factors related to the applicative details of the adopted NDT procedure.

In the present study, all the numerical simulations were carried out by the dedicated software CIVA^{nde} 10.1a [13]. The model was validated by simulating all the available experimental cases. In particular, Pictures 4a and 4b show the models built for the same sections already shown in Picture 3. As can be seen in Pictures 4c and 4d, the numerical results reasonably follow the experiments, allowing considering the adopted numerical procedure as validated and calibrated.

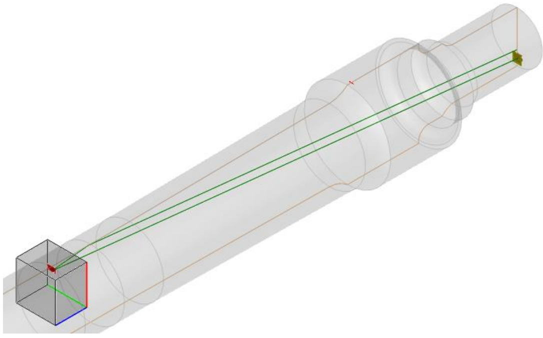

(a)

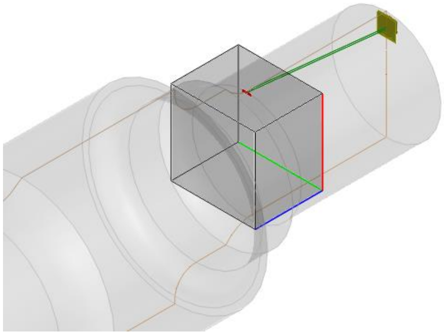

(b)

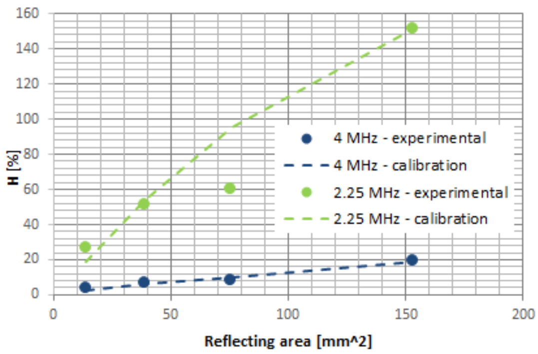

(c)

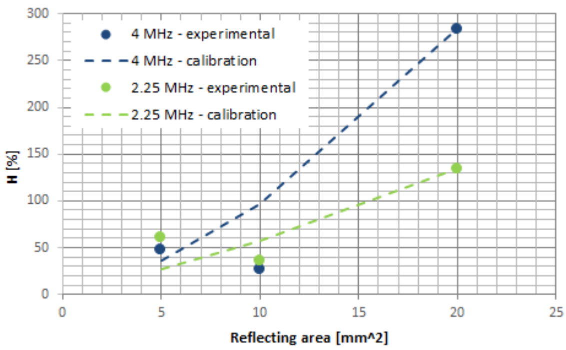

(d)

Pic. 4. Validation of the numerical model: a) and c) section B+E; b) and d) section G.

The numerical results shown in Picture 4 do not provide information about the inherent variability of the experimental ones, because they were obtained based on "ideal" conditions. The “complete” MAPOD approach [11] was then applied. In particular, the applied numerical procedure is essentially based on the Monte Carlo method: before each simulation, a value of the source (or sources) of variability is randomly extracted from the appropriate statistical distribution used to define the numerical set-up. In the end of all the programmed simulations, the obtained results should be reasonably representative of the effects of the selected source of variability on the results themselves.

Before going on, it is necessary to point out some peculiarities of the rotating probe. It is designed so that transducer can inspect an area of the axle different from the others and, therefore, every critical zone can be observed by only one of the available transducers. It can be concluded that the characterization of the reliability of the rotating probe consists in the collection of POD curves related to each transducer mounted in it. For simplicity, it will be analysed here, without losing generality in the description of the method, the performance of just the two sections (B + E and G) already considered in Pictures 3 and 4.

Picture 5 shows the results obtained for the two considered sections. In both cases, for brevity, only one source of variability was considered: the location of the defect along the longitudinal coordinate of the axle. Moreover, for both scenarios, such a position was characterized by a uniform statistical distribution. This was possible due to the following considerations:

- in the case of section B+E (Pic. 5a), the nucleation of fatigue cracks occurs in correspondence of in-service damages such as corrosion pits and impacts from ballast. It is not possible to predict the position of occurrence of such damages and, as a consequence, all the active sections of the axle should be described by the same probability of occurrence;

- in the case of section G (Fig. 5b), the damage occurs in terms of fretting-fatigue at the press-fit seat at a maximum distance of 20 mm from the edge of the press-fit. It is again not possible to provide a preferential position, but all those within the 20 mm will have the same chance of seeing the birth of a defect.

For each dimension of experimental artificial defect and for the two considered working frequencies (2.25 and 4 MHz), thirty random values of the source of variability were extracted and as many simulations were run, for a total of 240 simulations for section B+E (Pic. 5c and 5e) and 180 for the section G (Pic. 5d and 5f). The choice of thirty extractions for each scenario derives from the statistical theory that requires a minimum of 29 findings for the definition of the confidence band at 95%. The obtained results can then be used to derive the POD curves, remembering that the method can also be easily generalized to account for multiple sources of variability of the adopted inspection procedure.

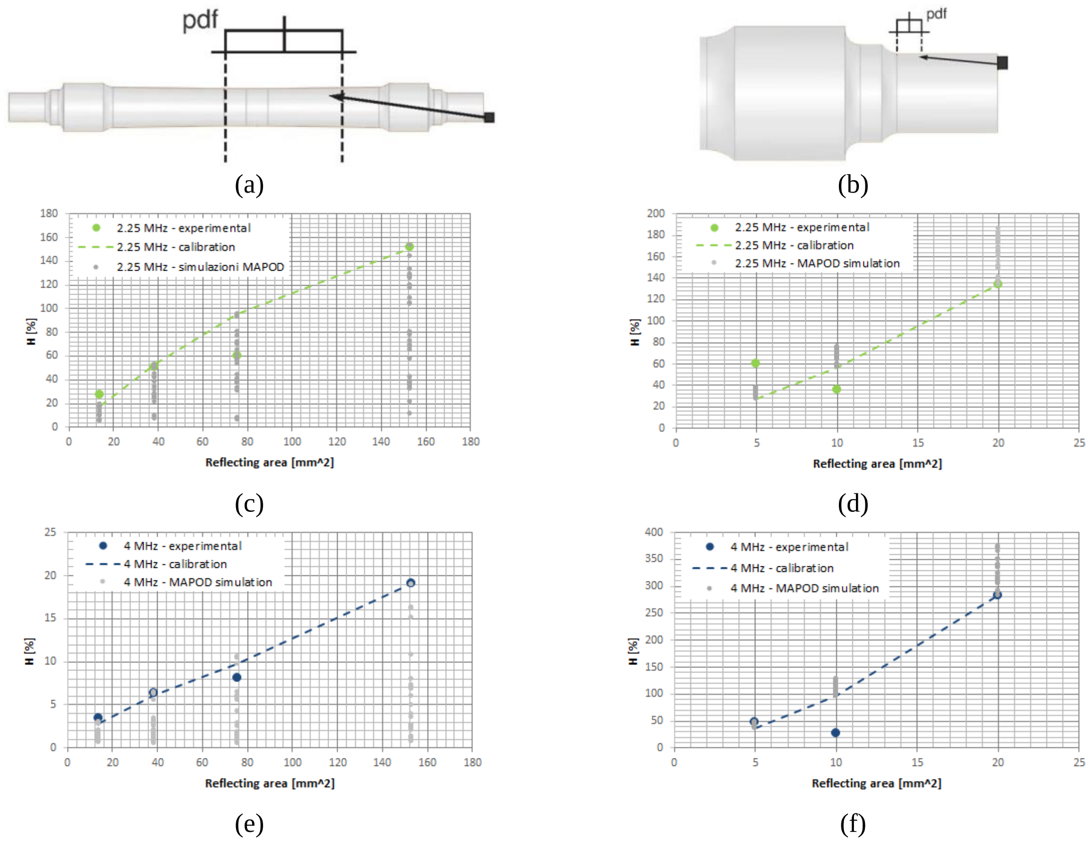

Pic. 5. MAPOD simulations: a), c) and e) section B+E; b), d) and f) section G.

4. Derivation of the POD Curve and Discussion

The “signal response” data shown in Picture 5 were mathematically elaborated by means of the Berens’ approach [8]. Generally speaking, a defect is considered as detected if its response exceeds some predefined decision threshold corresponding to the response of the defect to be detected with 50% probability [7]-[9]. The choice of the decision threshold is therefore one of the most critical points in the definition of POD curves. In this work, it was assumed equal to the value of the UT response obtained, by CIVA^{nde} simulations, from the sample defect defined in Lucchini’s procedure [6]. Picture 6 shows the analysis of the choice of the decision threshold on POD curves obtained from the experimental data shown in Picture 4. No confidence bands given due to the small available sample size.

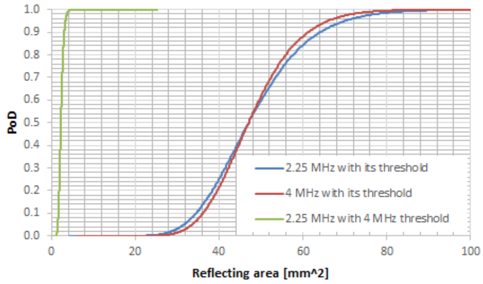

(a)

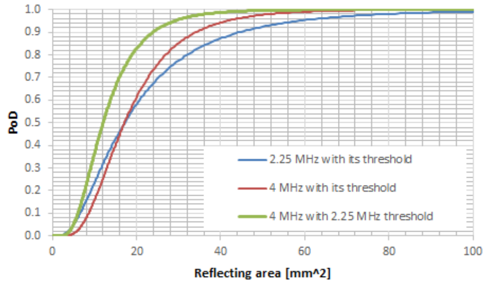

(b)

Pic. 6. Effect of the decision threshold for sections B+E (a) and G (b).

As can be seen for both the considered sections, the definition of the POD curve is equivalent when a data set is processed by the related decision threshold (i.e. the correct calibration). A piece of information was, however, lost during the construction of the POD curves: the absolute energetic difference of data set (see, for example, Picture 4c). Indeed, it is known that to responses of higher amplitude correspond, usually, signals and signal-to-noise ratios of better quality. To observe the influence of the energy content via the POD curves, it is necessary to implement a methodology (actually, not recommended and not applied in industrial practice) based on the use of the same decision threshold for all the available data sets, so to make them consistent with each other. In particular, the most suitable decision threshold should be the one of the data set with lower energy, but this would correspond to a calibration of the instrumentation based on a different sample defect, typically, too conservative. Picture 6 shows, however, this analysis as well, which leads to the same conclusions seen above: for long paths, a 2.25 MHz probe seems to be better, while for short ones, the 4 MHz probe seems better.

Considering, now, the MAPOD results of Picture 5, the relative MAPOD curves are compared to the corresponding experimental ones in Picture 7. The differences between numerical and experimental curves arise from the different number of data in each set and it is worth noting that all the curves pass through, at a probability of detection equal to 50%, the same point, corresponding to the decision threshold defined by the UT response of the calibration defect. Moreover, it can be noted that, in certain cases, the MAPOD curves show a better performance compared to the experimental POD one (Pic. 7b), in other cases worse (Pic. 7a). This suggests that the considered statistical variability is actually able to influence significantly the performance of the inspection procedure. On the other hand, this conclusion could have been drawn also from the results of Picture 5, where the experimental UT responses seem to lie on the upper limit of the numerical ones for section B+E and on the lower limit for section G. This information is now being used for both a further optimization of the sample defect and its position in the reference block.

5. Concluding Remarks

In the present study, the performance of the rotating probe applied to a particular geometry of solid axles made of EA1N and containing different types, sizes and locations of artificial defects obtained EDM was analysed. The obtained results showed that:

- the optimum frequency of inspection depends on the ultrasonic path: closer defects seem to be better detected by a 4 MHz probe, while farther ones by a 2.25 MHz one;
- the decision threshold for the definition of the POD curves is a critical parameter and should be chosen contextually to the definition of the reference block;

- numerically speaking, taking into account the statistical variability of the inspection procedure, a description of the performance of the rotating probe significantly different from the one obtained by a few experimental values was obtained.

Further investigations on a larger experimental sample are now being done in order to better characterize the obtained results.

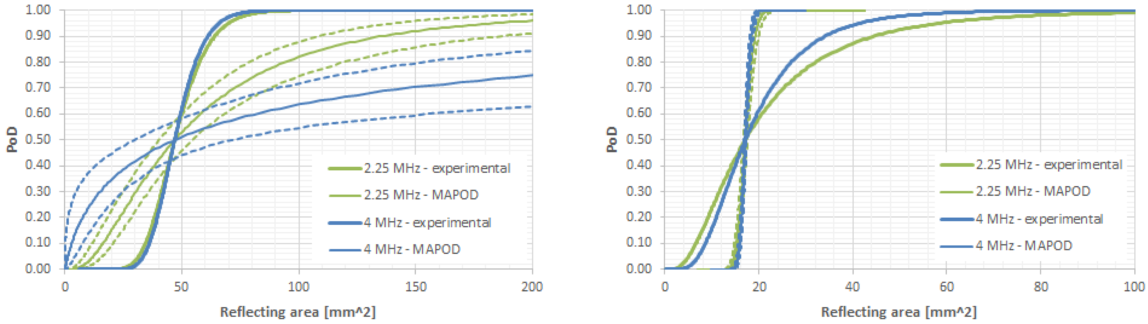

(a) (b)

Pic. 7. MAPOD curves for sections B+E (a) and G (b).

References

[1] VPI, VPI 04 – Maintenance of freight trains – Wheel-sets, 2° edition, 1° modification, valid from 01/08/2008.

[2] S. Cervello, D. Sala, LURSAK: Developement of Innovative anti impact coating return from experience, Proc. 17th International Wheelset Congress, Kiev, 2013.

[3] S. Cantini, S. Beretta (Editors), Structural reliability assessment of railway axles, LRS-Techno Series 4, 2011.

[4] Grandt AF Jr. Fundamentals of structural integrity. John Wiley & Sons Inc., Hoboken, 2003.

[5] G. Pettinato, Il controllo ad ultrasuoni semiautomatico degli assi delle sale montate dei veicoli ferroviari in opera o fuori opera, La Metallurgia Italiana 8, 1971.

[6] F. Benzoni, S. Cantini, L. Tonelli, Istruzione Tecnica QUA IT 142 Rev.1. 2013, Lucchini RS S.p.A., Lovere (BG).

[7] Georgiou GA. Probability of Detection (POD) curves: derivation, applications and limitations. Research Report 454, HSE Books, Health and Safety, Executive, UK, 2006.

[8] ASM. ASM handbook – Vol. 17: Non-destructive evaluation and quality control. 1997.

[9] MIL-HDBK-1823A. Nondestructive evaluation system reliability assessment. Department of Defense of the US, 2009.

[10] http://www.cnde.iastate.edu/MAPOD/index.htm.

[11] R.B. Thompson, L. Brasche, J. Knopp, J. Malas, 'Use of physics-based models of inspection processes to assist in determining probability of detection', Proc. Aging Aircraft Conference, 2006.

[12] J.S. Knopp, J.C. Aldrin, E. Lindgren, C. Annis, 'Investigation of a model-assisted approach to probability of detection evaluation', AFRL-ML-WP-TP-2006-494 Report, AIR FORCE RESEARCH LABORATORY, 2006.

[13] CEDRAT, CIVAnde 10.1a User's Manual, 2013.

[14] Carboni M. (2012), A critical analysis of ultrasonic echoes coming from natural and artificial flaws and its implications in the derivation of probability of detection curves, Insight 54, 208-216.